Clustering and phases of compartmentalized granular gases

K. C. Chen, C. C. Li, C. H. Lin, and G. H. Guo
Institute of Applied Mechanics, National Taiwan University, Taipei 106, Taiwan, Republic of China
(Received 4 September 2008; revised manuscript received 26 January 2009; published 27 February 2009)

This paper experimentally investigates the clustering conditions for compartmentalized monodisperse granular gases, determining the critical particle number and condensation granular temperature at the gas-clustering transition. When one heavier intruding particle is added to a monodisperse gas, it is found that the condensation temperature decreases with the ratio of the mass of the intruding particle to that of the background particle. This phenomenon can be mathematically characterized by a proposed linear relation, which is reminiscent of a relation between the freezing point depression for a solvent and the concentration of an added solute. Finally we perform various tests by changing the numbers of two types of particles in bidisperse granular mixtures to construct the phase diagrams, which present the range of the five different states, namely, homogeneous gas, unstable-gas, one-clustering, two-clustering, and granular oscillation states.

DOI: 10.1103/PhysRevE.79.021307 PACS number(s): 45.70.Mg, 45.70.Vn, 05.65.+b, 47.54.−r

I. INTRODUCTION

Granular materials play an important role in various academic and industrial activities and fields, including geophysics, geology, geotechnical engineering, pharmaceutics, powder metallurgy, and ground mining [1–5]. When granular materials remain in a gaseous state, the most peculiar feature that differentiates them from molecular gases is their tendency to form highly concentrated and dilute regions [1,6,7]. This clustering, showing its diversity particularly in a vertically oscillated compartmentalized system [8–14], originates from the dissipation of energy from inelastic collisions between granular particles. Recent studies show that the clustering in a compartmentalized bidisperse granular system is able to oscillate as soon as moderate energy is imposed on the system [15–18]. This oscillation is either called "granular clock" for a two-compartment container or more generally called "granular follower" for a multicompartment container [19]. Experimental evidence shows that granular oscillation comprises a series of two-stage performance: in stage I lighter particles (LPs) are expelled by heavier particles (HPs) and in stage II HPs follow LPs[19].

Researchers have investigated the subject of granular oscillation using several approaches: (i) numerical studies that employ two-dimensional (2D) molecular dynamics (MD) simulation [15,16] or that simulate the proposed phenomenological flux modeling [18], (ii) experimental verifications in a quasi-2D test with two types of particles of different sizes [17] or in a 3D test with two types of particles of the same size [18], and (iii) theoretical treatment through kinetic theory of gas [15]. These studies all contribute to a basic knowledge of granular oscillation, and indicate that this oscillation behavior occurs within a limited range of parameters, such as input energy, container geometry, and the number and diameter of particles. In spite of these contributions, there are still several unsolved issues that require detailed investigation. These issues include the verification of temperature-driven mechanism of granular oscillation [18], the requirements for generating the oscillation, and the construction of a complete phase diagram in the particle numbers of LPs and HPs.

Since cluster formation of LPs in an empty compartment is a necessary condition for generating the granular oscillation of a bidisperse gas in stage I, where LPs are expelled by HPs [19], it is necessary to have a better understanding of the critical conditions for the clustering of compartmentalized granular gases. For cluster formation in compartmentalized granular gases, several excellent works have been completed over the past decade, such as the Maxwell-demon experiment [9,20] and the bifurcation analysis [5,8,21]. According to these studies, the symmetry breaking in compartmentalized granular gases can be analytically interpreted by the phenomenological flux model [8] and by the hydrodynamic treatment [21].

Concentrating on the conditions for generating granular oscillation and the related temperature issue, this paper performs three main tasks. First, the clustering conditions of a monodisperse gas under different container geometric factors are investigated by measuring the critical particle number at the gas-clustering transition. Each critical particle number is experimentally obtained from a bifurcation diagram, i.e., the relation between the input energy and the particle proportion in each compartment. By using the flux model, we deduce the condensation granular temperature of a monodisperse gas from this critical number information. Second, this study extends the analysis to an "$M+1$" gas, which is defined here as a gas composed of a monodisperse gas and an intruding larger particle. Results show that the condensation temperature changes with the mass of the additional particle, and this change is reminiscent of the freezing point depression that results from adding a small amount of solute into a solvent [22]. Third, we construct the phase diagram in the numbers of heavier and lighter particles, showing that there are five states for a bidisperse two-compartmentalized system, i.e., homogeneous gas, unstable gas, one-clustering, two-clustering, and granular oscillation states. The final section summarizes the findings of this study.

II. EXPERIMENTAL DETAILS

Our experimental setup consists of nine acrylic containers in rectangular shape (total height $H=15.4$ cm) with various

TABLE I. Geometric factors of acrylic containers used in the experiments.

Container (Symbol)	N_c	W (mm)	D (mm)	h (mm)
$C1(\bigcirc)$	3	22	7.5	30
$C2(\times)$	2	22	7.5	30
$C3(\Delta)$	2	35.5	7.5	30
$C4(*)$	4	22	7.5	30
$C5(\square)$	3	22	5.5	30
$C6(\diamond)$	3	22	9.5	30
$C7(+)$	3	22	11.5	30
$C8(\star)$	3	22	7.5	35
$C9(\triangledown)$	3	22	7.5	40

combinations of geometric factors (number of compartments N_c, compartment width W, container depth D, and barrier height h), as presented in Table I. These containers with equally divided two, three, or four compartments in the width direction are tightly mounted on a shaker (VTS-65, Aurora), which offers a vertical and sinusoidal oscillation. The shaker's frequency f is fixed at 20 Hz and its amplitude is adjustable through the input signal controlled by a function generator (SFG-2004, Good Will Instrument) and magnified by an amplify (CE 1000, Harman International). The input energy is represented by the dimensionless acceleration $\Gamma(=4a\pi^2f^2/g)$, where g denotes the gravitational acceleration, and the output acceleration of the containers is monitored by an accelerometer (ProBall II General Balancer). The following sections provide details on the spherical particles used in each test.

III. PARTICLE NUMBER AND GRANULAR TEMPERATURE FOR CLUSTERING OF MONODISPERSE GASES

Most attention of the Maxwell-demon experiments has been given to the construction of the bifurcation diagram, exhibiting the relation between input energy and particle number in each compartment. This study will take a further step to obtain, from the bifurcation diagram, the critical granular temperature at the phase transition between the granular-gas state and the clustering state.

We begin the study of cluster formation from the construction of the relation between input energy and particle proportion in each compartment for a monodisperse gas. Figure 1 shows the experimental results for (a) the two-compartment (2C) system, i.e., 65 steel balls of 2 mm diameter in container $C2$, and (b) the three-compartment (3C) system, i.e., 100 steel balls of 2 mm diameter in container $C1$. Each point in Fig. 1 is obtained by recording the particle number in each compartment after the system is subjected to a specific Γ value for 30 s and then returns to a static condition. The value Γ was set in a decreasing manner from a value greater than 12, or was set in an increasing manner from zero. The chosen 30-s period was not critical for the final record because we found that all the test for 15, 30, and

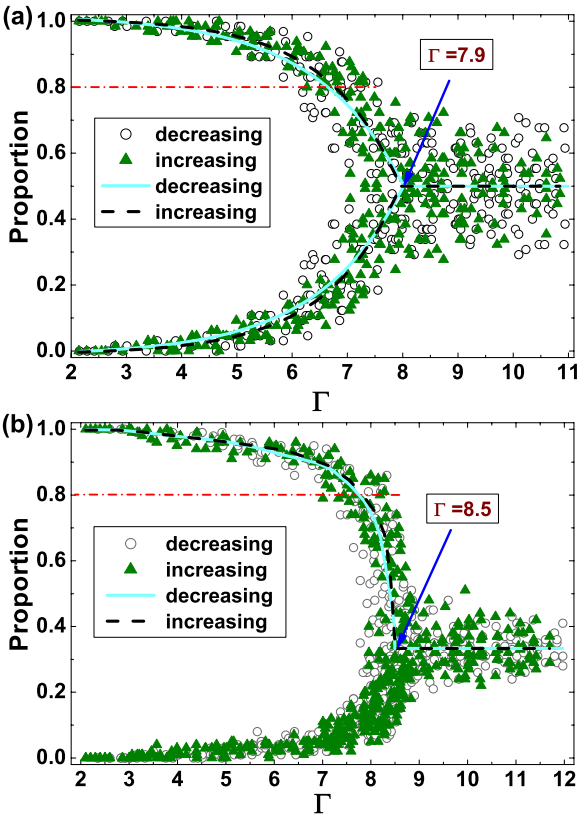

FIG. 1. (Color online) Bifurcation diagrams for the two systems: (a) 65 steel balls of 2 mm diameter in container $C2$ and (b) 100 steel balls of 2 mm diameter in container $C1$. The data points represented by the circles "○" are obtained by decreasing Γ from $\Gamma > 12$ and the triangles "▲" are obtained by increasing Γ from $\Gamma = 0$. The decreasing and increasing lines in each diagram, which are obtained from an approximate average of each circular and triangle point, respectively, almost overlap with each other, showing the nonhysteretic nature of the two systems. The phase transition between granular gas and clustering states is defined as the moment when 80% of particles cluster in one compartment.

60 s, respectively, resulted in the same particle distribution. Figure 1 shows that no obvious hysteretic phenomena can be observed in the 2C and 3C systems, which is different from the experimental finding of van der Weele *et al.* [9] that the cyclic three-box system exhibits a hysteretic bifurcation. The reason for this difference could be attributed to the noncyclic compartments for our 3C system.

As also illustrated in Fig. 1, there does not exist a sharp transition between granular-gas and clustering states; the former state refers to one in which particles are randomly distributed in all compartments, and the latter to one in which particles form a cluster in one compartment. Based on our preliminary experimental observation that a cluster of 80% of the particles in the dynamical situation is more stable and easier to distinguish from a cluster composed of smaller proportion of particles, we define the gas-clustering phase transition as the moment when 80% of the particles cluster in one zone. With this definition, we perform a sequence of tests that measure the critical particle number of a monodisperse gas at the gas-clustering transition. In each test with fixed input energy, particles are added one by one into the

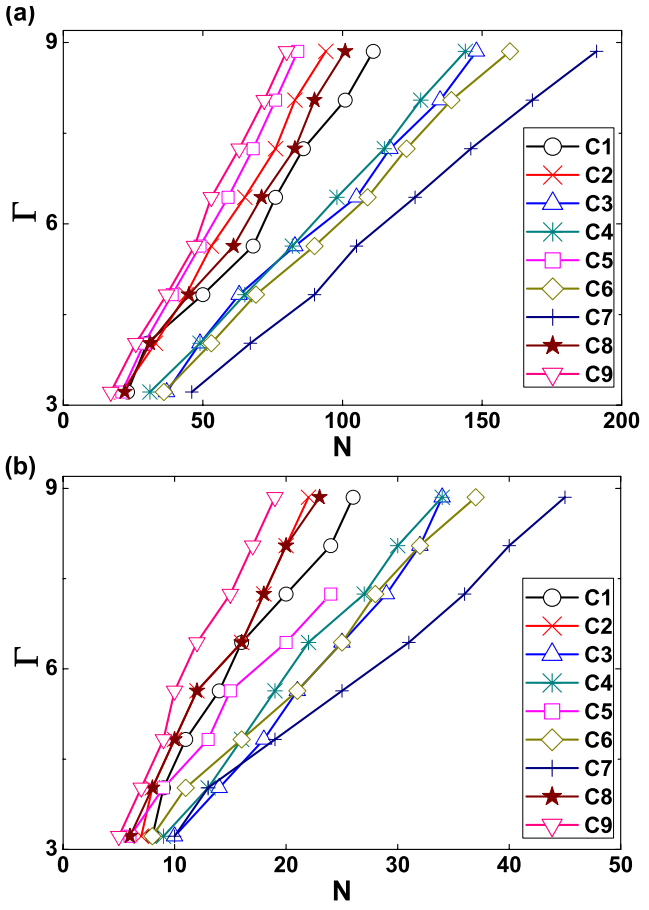

FIG. 2. (Color online) Relations between the input energy and critical particle numbers for monodisperse gases from a granular-gas state to a clustering state. Two kinds of gases with steel balls of (a) 2 and (b) 4 mm in diameter are presented here. Different symbols represent different containers.

compartmentalized system until they shift from a granular-gas state to a clustering state. To assure the critical value of particle number for each test, we conduct five times to obtain their average. The test particles are spherical steel balls of 1.5, 2, 3, and 4 mm in diameter.

Let N denote particle number. Figure 2 shows the relations between the input energy and the critical particle number for various container factors and particle diameters, where each data point in Γ-N space is obtained from one bifurcation diagram. In Fig. 2 each curve depicts the minimum number of particles required to form a cluster. The right-hand side of each curve represents the domain of the clustering states, and the left-hand side that of the granular-gas states. The subfigure identifies the size of the steel balls used in the tests: (a) for 2 mm and (b) for 4 mm, and each symbol represents the type of container indicated in Table I. The energy-particle number relations obtained by using steel balls of 1.5 and 3 mm, which are not shown in the figure for simplicity, share the same pattern with that in Fig. 2(a), i.e., from left to right: $C9 \rightarrow C5 \rightarrow C2 \rightarrow C8 \rightarrow C1 \rightarrow C4 \rightarrow C3 \rightarrow C6 \rightarrow C7$. However, the case of 4-mm particles in container $C5$ deviates from this pattern, as shown in Fig. 2(b). This deviation could be explained by the fact that the small ratio of container depth to particle diameter reduces the frequency of collisions, which leads to an increase in particle number for clustering.

We observe from Fig. 2 that cluster formation requires more particles as the particle size decreases. This is due to the fact that the collision frequency for small-size particles is lower than that for large-size particles under the same container, particle number, and input energy, which results in more particles required to dissipate energy in a small-size particle system. In addition, Fig. 2 reveals the following features that (i) with the same Γ, N_c, W, and D, the higher the barrier, the fewer the particles are required for clustering; (ii) with the same Γ, W, D, and h, the greater the number of compartments, the greater the particle number required for clustering; and (iii) when the values of the bottom areas of two containers are close to each other, the greater the number of compartments, the lower the particle number is required for clustering.

The experimental data reveals not only the critical particle number at the phase transition between granular-gas state and clustering state of a monodisperse granular gas, but is also able to provide useful information of this transition while incorporating this data into an existing analytical approach. In the past, two elegant analytical approaches have been proposed to study the feature of cluster formation in compartmentalized granular gases, i.e., the flux model [8] and the hydrodynamic treatment [21,23]. The basic difference between the two approaches is that in the flux model, the temperature T is constant and the pressure p is changed along the direction of container height; conversely, in the hydrodynamic treatment, p is constant and T is changeable with the distance from the vibrating wall. However, both treatments have introduced a nonmonotonic function termed $\hat{F}^E(n)$ in the flux model characterizing the particle flux, and termed $\hat{F}^B(\xi)$ in the hydrodynamic approach characterizing the pressure, such that it is possible to find $\hat{F}^E(n_l)=\hat{F}^E(n_r)$ [or $\hat{F}^B(\xi_l)=\hat{F}^B(\xi_r)$] with $n_l \neq n_r$ (or $\xi_l \neq \xi_r$) in a steady state. Here, n_l (n_r) denotes the fraction of the total particle number in the left (right) compartment, and ξ refers to the dimensionless parameter, related to the particle number.

In order to explore the critical granular temperature, this study follows the flux-model approach [12,13], and adopts two assumptions for a monodisperse gas in granular-gas state: (i) the particle number distribution obeys the barometric height relation and (ii) the velocity distribution of particles is Maxwellian and isotropic [13]. The barometric relation is the result of the ideal gas law, $p=nk_BT$, and the condition that the temperature T is independent of z, where z is the position measured upwards from the container bottom. The first assumption implies that the number density n decays exponentially with the z direction, i.e., $n(z)=n(0)\exp(-mgz/T)$, where m is the particle mass. Based on this assumption and the condition $\Omega\int_0^H n(z)dz=N$, we obtain $n(0)=mgN\zeta_1/\Omega T$, where $\Omega(=N_cWD)$ is the total of the bottom areas of the compartments and the factor ζ_1 is given by $\zeta_1=[1-\exp(-mgH/T)]^{-1}$. When $H\rightarrow\infty$ and g is finite, we have $g\zeta_1\rightarrow g$; whereas we have $g\zeta_1\rightarrow T/mH$ when $g\rightarrow 0$ and H is finite. The second assumption allows us to associate the z component of the particle velocity $\mathbf{v}$ with the granular temperature T of the system through the relation $\langle v_z^2\rangle=\frac{1}{3}\langle v^2\rangle$

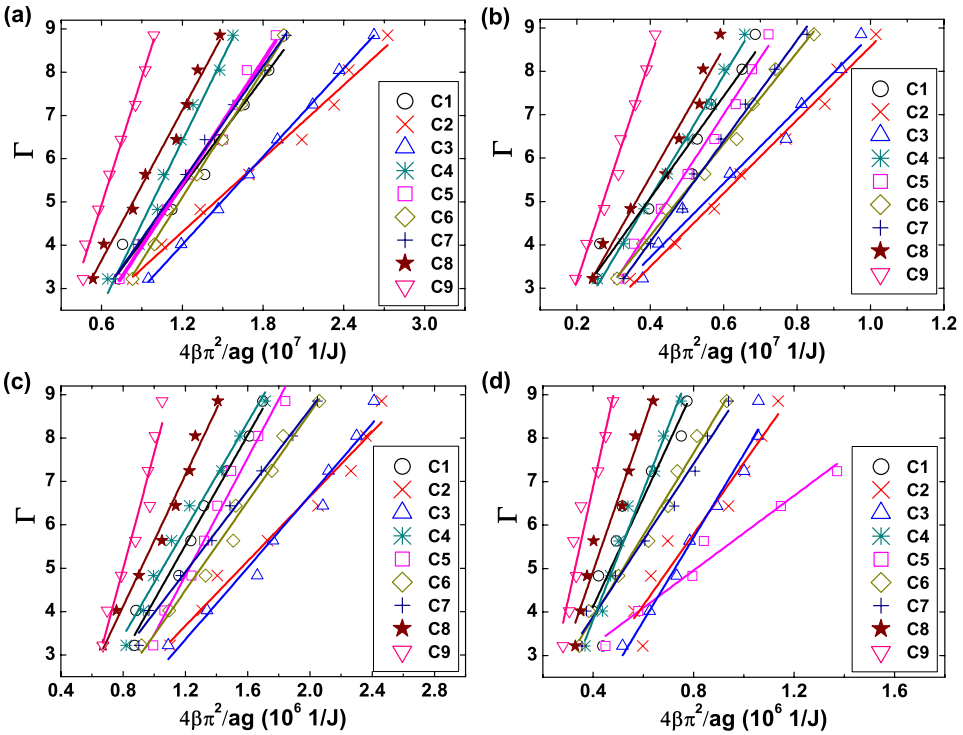

FIG. 3. (Color online) Gas-clustering transitions in terms of the dimensionless acceleration Γ and the quantity $4\beta\pi^2/ag$ for the four gases: (a) 1.5, (b) 2, (c) 3, and (d) 4 mm. The transition for each gas in various containers is mathematically characterized by a linear curve.

$=k_BT/m$, where the Boltzmann constant k_B will be taken to be 1 in the following analysis. It should be noted that even if the two assumptions have been shown to be invalid [24], the exponential distribution and the equal temperature components roughly hold from molecular dynamics simulations of a vertically vibrated granular gas [13]. Thus, the two assumptions are only treated as a first approximation.

For simplicity, we assume that the restitution coefficients of collisions between particle and particle e_p and between particle and container bottom e_w are equal, i.e., $e_p=e_w=e$. We also assume a sawtooth motion of the container bottom such that the container bottom has the upward velocity $v_b=af$ (a: shaker's amplitude; f: shaker's frequency) as it collides inelastically with particles [8,13]. Accounting for the energies involved in a single particle-particle and container bottom-particle collision [12,13], we are thus led to the rate of input energy

$$J_0 = -(1-e^2)g\zeta_1 N\sqrt{\frac{mT}{2\pi}} + \frac{1}{2}e(1+e)v_b mg\zeta_1 N \qquad (1)$$

and the rate of energy dissipation

$$Q = \frac{(1-e^2)d^2 g\zeta_2 N^2\sqrt{\pi mT}}{\Omega}, \qquad (2)$$

where ζ_2 is given by $\zeta_2=[1-\exp(-2mgH/T)]^{-1}$, and d and ρ are the particle diameter and mass density of particle, respectively. In a special situation without gravity, i.e., $g=0$ ($\zeta_1,\zeta_2\to\infty$), the energy injection and dissipation expressed in Eqs. (1) and (2) will not vanish and approach certain values [21,23]. In the presence of gravity, we assume without loss of generality that both ζ_1 and ζ_2 are 1. If the rate of energy dissipation from particle-particle collision is balanced by the rate of input energy supplied by container bottom-particle collision for a monodisperse granular gas in granular-gas state, i.e., $J_0=Q$, then

$$\frac{\Gamma}{T} = \frac{4\beta\pi^2}{ag}, \qquad (3)$$

where

$$\beta = \frac{24(1-e)^2}{e^2\rho\pi d^3}\left(\frac{\sqrt{\pi}}{\Omega}d^2N + \frac{1}{\sqrt{2\pi}}\right)^2 \qquad (4)$$

is a quantity, characterizing the ratio of the input energy and the system's kinetic energy. In the ideal case of elastic collision, $e=1$ gives rise to $\beta=0$, which implies $T\to\infty$, i.e., the energy of the system increases continuously.

With the help of Eq. (3), replace the measure of the x axis, i.e., particle number, in Fig. 2 by the quantity $4\beta\pi^2/ag$, where the restitution coefficient is given by $e=0.88$ as obtained from a drop test. Figure 3 displays the resulting experimental phase diagram of the gas-clustering transition, which shows that for each case the transition is described by a linear curve with a slope, having the physical meaning of granular temperature T. As in Fig. 2, the left side of each curve represents the domain of granular-gas states, while clustering states appear on the right side. In the procedure of adding particles to the system, the granular-gas state of the monodisperse gas evolves horizontally to the right until the particles cluster. Specifically, as the number of particles increases steadily, the granular temperature of the gas continuously decreases to the critical temperature where the gas condenses.

Figure 3 shows that the granular temperature at the gas-clustering transition, called the condensation temperature T_c, increases as the particle diameter increases. This is obvious since a particle with a larger diameter has a greater mass,

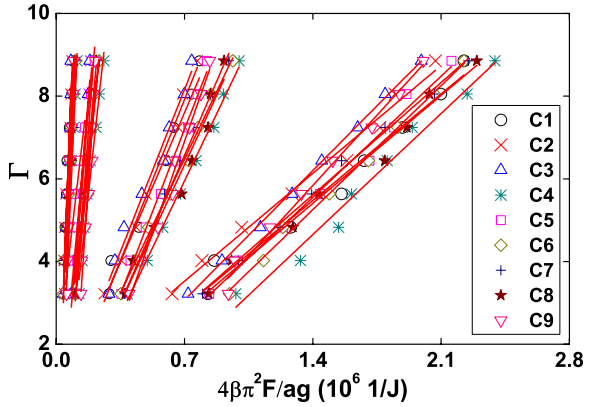

FIG. 4. (Color online) Gas-clustering transitions in terms of Γ and $4\beta\pi^2F/ag$. The results obtained from the nine different containers for each gas are merged into a group of straight lines, having almost the same slope within the test range of input energy. Four groups, respectively, represent the gases with steel balls of 1.5, 2, 3, and 4 mm from right to left.

leading to a higher kinetic energy. For a specific monodisperse gas, Fig. 3 reveals several interesting experimental findings. (i) Except for the case of 4 mm particles in a 5.5-mm-deep container, the orders in the magnitude of temperature in the nine containers are almost the same for each granular gas. (ii) A higher barrier, which more easily constrains the motion of particles within a compartment, leads to a higher condensation temperature (see samples C1, C8, and C9 with the same N_c, W, and D). (iii) Comparing samples C5 and C7 shows that container depth has little effect on the transition temperature. (iv) With the same compartment width as in samples C1, C2, and C4, particles in a container with more compartments will cluster at a higher granular temperature. (v) Under the same barrier height and approximately the same total compartment bottom area Ω, the system with more compartments has a higher granular temperature at the transition (see samples C1 and C3, samples C2 and C5, or samples C4 and C6).

To aggregate various cases of different container geometric factors as a group, an additional dimensionless parameter $F[=N_c(h/H)^2]$ is introduced to accompany the quantity β. Figure 4, which uses $4\beta\pi^2F/ag$ as the measure of the x axis, displays an approximately common slope $T/F(=\Gamma ag/4\beta\pi^2F)$, for each granular gas in different containers within our test range of input energy. Four groups with increasing order in their slopes correspond to gases with steel balls of 1.5, 2, 3, and 4 mm. According to Fig. 4, a greater number of compartments and a higher barrier height both contribute to a higher gas-clustering transition temperature given a fixed particle number and total area of the compartment bottom.

IV. CLUSTERING OF THE $M+I1$ GASES

The phenomena involved in compartmentalized bidisperse gases are much more complex than those in monodisperse gases since different sizes or materials lead to more complicated interactions between particles. Research on this subject can begin simply with an experimental investigation on change in critical particle number at the gas-clustering transition while adding one intruding particle into a monodisperse gas. This experiment uses the container $C2$ and performs the transition test on the $M+I1$ gases, whose the background particles of 2 mm in diameter can be glass beads or steel balls, and the intruding particle of 4 mm in diameter is polypropene ball, nylon ball, glass bead, steel ball, or bronze ball. Table II lists the mass density ρ and restitution coefficient e of various particles used in this test.

TABLE II. Some material properties of the particles used in the test.

Property	Polypropene	Nylon	Glass	Steel	Bronze
ρ[g/cm^3]	0.9	1.14	2.50	7.92	8.90
e	0.9	0.95	0.92	0.88	0.78

For a monodisperse gas of 2-mm-glass beads, Fig. 5(a) shows that adding one glass bead, steel ball, or bronze ball of 4 mm decreases the input acceleration (or energy) required

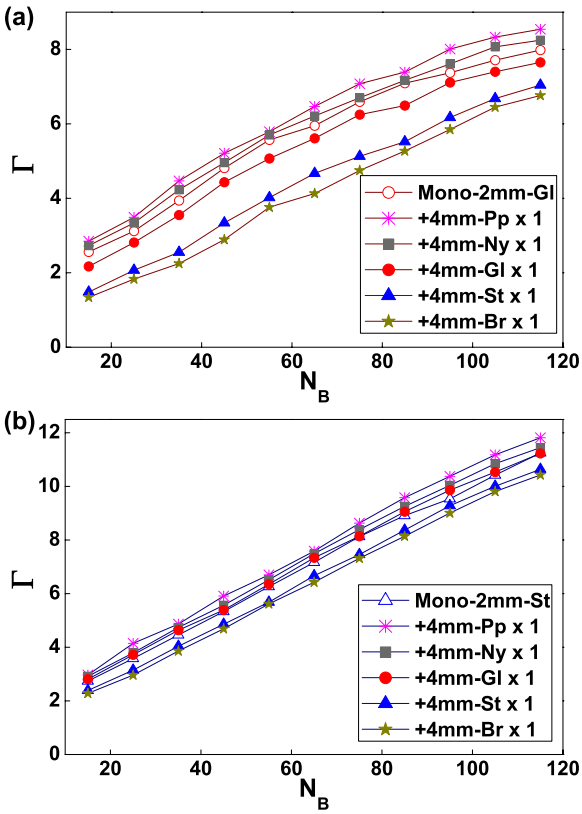

FIG. 5. (Color online) Relation between input acceleration Γ and number of background particles N_B at the gas-clustering transition for the $M+I1$ gases, whose background particles are (a) 2-mm-glass beads and (b) 2-mm-steel balls. The original gases are monodisperse, denoted by ○ and △, are added by one 4 mm intruding particle, which can be polypropene (Pp) ball, nylon (Ny) ball, glass (Gl) bead, steel (St) ball, or bronze (Br) ball. Likewise, the left side of each curve represents a domain of granular-gas states, while clustering states are on the right side.

for generating the gas-clustering transition. A heavier intruding particle (4-mm-bronze ball) causes a more pronounced decrease than a lighter intruding particle (4-mm glass bead or steel ball). However, this decrease changes to an increase when adding a polypropene or nylon ball. Figure 5(b) shows a similar result where the background particles are 2-mm steel balls. This change in input energy is due to the fact that a heavier particle with a larger mass has a larger kinetic energy. Along with it comes an increase in inelastic collisions in the system, causing the gas-clustering transition to occur at a lower input energy.

Section III showed that each curve in the Γ-N space, representing the set of the critical points for the gas-clustering transition, is associated with the T_c of a monodisperse gas. In view of the granular temperature perspective, adding a larger and heavier particle will result in a change (decrease or increase) in T_c, depending on the size, mass, and material property of the intruding particle. This change is attributed to the difference between the kinetic energy and dissipation energy arising from the intruding particle, and is presumably dominated by the mass ratio μ and the restitution coefficients between particles. Here, μ is defined as the mass of the intruding particle m^I divided by the mass of a single background particle m^M. The experimental results in Fig. 5 implicitly suggest that T_c decreases when μ exceeds a certain threshold value μ_{th}.

The phenomenon of a decrease in T_c of the granular gas is reminiscent of the freezing point depression when a small amount of solute is added to a pure solvent [22]. This depression ΔT_f is determined by the relation $\Delta T_f = K_f c_b$, where K_f and c_b are the cryoscopic constant and the concentration of a solution, respectively. With reference to this relation, we predict that the change in condensation temperature ΔT_c can be approximately given as

$$\Delta T_c = K_c(\mu - \mu_{\text{th}}), \tag{5}$$

where μ_{th} is the threshold mass ratio and K_c is a proportional parameter. To confirm the validity of the prediction, we adopt a hypothesis, which is similar to that employed in Sec. III, that for a bidisperse granular gas, $Q = J_0$ holds at the granular gas state. This hypothesis helps to extend Eq. (3) to

$$(af)^2 = \frac{4T(1-e)^2}{e^2(m_1N_1 + m_2N_2)^2}\left(\frac{\sqrt{\pi}\alpha}{\Omega} + \frac{\sqrt{m_1}N_1 + \sqrt{m_2}N_2}{\sqrt{2\pi}}\right)^2 \tag{6}$$

for a bidisperse gas (which also hold for an $M+I1$ gas), where

$$\alpha = d_1^2N_1^2\sqrt{m_1} + d_2^2N_2^2\sqrt{m_2} + \frac{(d_1+d_2)^2N_1N_2\sqrt{m_1m_2(m_1+m_2)}}{\sqrt{2}(m_1+m_2)}, \tag{7}$$

with m_i, N_i, and d_i being the mass, number, and diameter of the i-kind particle, respectively ($i=1$ or 2).

The above derivation has assumed that restitution coefficients for all collisions are equal to the same value e and that the granular temperatures for both kinds of particles are the same. Note, however, that equipartition of energy in bidisperse granular gases has been proved to be invalid, i.e., two particle species have their own granular temperatures [25,26], and the nonequipartition is strongly dependent on the restitution coefficient and mass difference between particles [27]. But since we focus on how one single intruding large particle into a monodisperse gas influences the averaged temperature of all particles, for simplicity of analysis, we still take the assumption that the temperatures are the same and treat it only as an approximation.

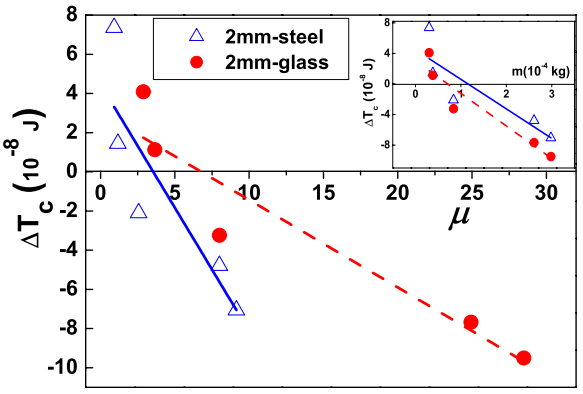

FIG. 6. (Color online) Linear approximation for the change in condensation temperature $\Delta T_c (= T_c^I - T_c^M)$, and the mass ratio of intruding and background particles $\mu (= m^I/m^M)$. Two types of background particles, namely, 2-mm-glass beads and 2-mm-steel balls, are adopted. Every T_c can be obtained in view of Eq. (6).

Using Eq. (6), we evaluate the T_c's for those gases indicated by the curves in Figs. 5(a) and 5(b). Let us classify these gases into $G2$ type and S2 type, where the $G2$ type, represented by the symbol "●" in Fig. 6, refers to the gases whose background particles are 2-mm glass beads. Those gases with background particles of 2-mm steel balls belong to the S2 type, denoted by "△." Figure 6 presents the linear curve-fitting relation between $\Delta T_c (= T_c^I - T_c^M)$ and the mass ratio μ for each type of gas, where T_c^I and T_c^M are the two T_c's for a monodisperse gas with and without one intruding particle, respectively. The two linear curves in Fig. 6, corresponding to Eq. (5), reveal that $K_c = -4.46 \times 10^{-9}$ J and $\mu_{\text{th}} = 6.78$ for the $G2$-type gases, and $K_c = -1.26 \times 10^{-8}$ J and $\mu_{\text{th}} = 3.55$ for the S2-type gases. If we change the measure of the x axis from the mass ratio to the mass of intruding particle, then the two straight lines, corresponding to the two types of gases, can be obtained as also illustrated in Fig. 6, which shows that the magnitude of change in T_c depends on the mass of the intruding particle. Besides, the difference in the threshold masses, indicated by the intercepts, should come from the different natures of the background particles.

V. PHASE DIAGRAMS OF COMPARTMENTALIZED BIDISPERSE GRANULAR GASES

A compartmentalized bidisperse granular gas exhibits several extraordinary phenomena, including granular oscillation, which are not easily explained by directly modifying the data collected from a monodisperse gas. Based on experimental observations, granular oscillation can take place if the following requirements are satisfied: (I) LPs can be expelled by

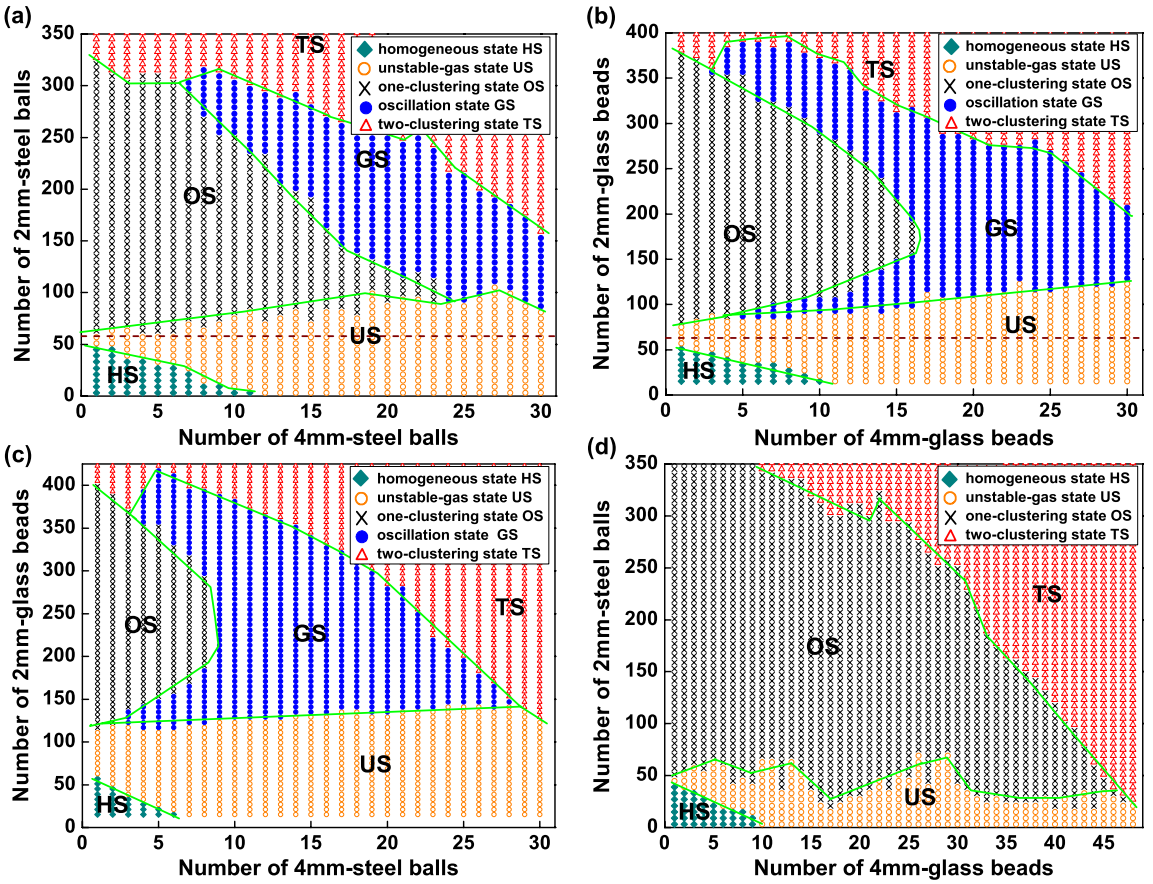

FIG. 7. (Color online) Phase diagrams in the particle numbers of (a) 2-mm-steel balls versus 4-mm-steel balls ($\bar{\mu}=8$), (b) 2-mm-glass beads versus 4-mm-glass beads ($\bar{\mu}=8$), (c) 2-mm-glass beads versus 4-mm-steel balls ($\bar{\mu}=25.34$), and (d) 2-mm-steel balls versus 4-mm-glass beads ($\bar{\mu}=2.53$), where $\bar{\mu}$ is the ratio for masses of a single heavier and a single lighter particles. The domain is primarily divided by HS, US, OS, GS, and TS. The horizontal dash line indicates a borderline, above which the monodisperse gas comprised of LPs can cluster in one compartment.

HPs, (II) LPs can cluster in an empty compartment, and (III) HPs can be trapped by LPs (the abbreviations for HPs and LPs have been noted in Sec. I). The Brazil nut (BN) effect or reverse Brazil nut (RBN) effect is not necessarily responsible for this oscillation [18,19].

To illustrate the conditions for generating granular oscillation, we present four phase diagrams in the N_H-N_L space as shown in Fig. 7, where N_H and N_L represent the numbers of HPs and LPs, respectively. The heavier particles are 4-mm glass beads or steel balls, whereas the lighter particles refer to those in 2 mm. By using the container $C2$ and keeping $\Gamma=6.44$ ($a=4$ mm) fixed, we conduct a series of tests to record the final state for each combination of N_H and N_L after a 3-min period of oscillation. The initial state for each test is to randomly deposit the particles, since we found that changing any initial state has no influence on the final state. Each diagram in Fig. 7 is constructed by all experimental data points, which are obtained by adding LPs three by three into the system, each time with a specific number of HPs. Because the same final state can be also obtained by changing the procedure either by decreasing the number of LPs (e.g., from 350, 347, downward) or by adding HPs one by one into the system with a specific number of LPs, it is concluded that no hysteresis can be found between any two states.

Figure 7 displays five states of each binary mixture as well as a dash line, called a "clustering line," that indicates the minimum particle number required for the corresponding monodisperse gas of LPs to cluster in an empty compartment ($N_L=63$ for 2-mm glass beads and $N_L=58$ for 2-mm steel balls). The five states are described below.

(i) *Homogeneous-gas state (HS)*. In a dynamical situation, with small numbers of HPs and LPs, particles randomly distribute themselves within the two compartments. In this state, it is difficult to observe the difference of particle proportions between the two compartments within a 3-min period, i.e., particle numbers in the two compartments are statistically the same and no clustering tendency for particles can be found. However, as soon as one turns off the shaker, a deviation from the mean particle number is possible. The HS state is analogous to the granular-gas state for $\Gamma>7.9$ in Fig. 1(a), where the values of particle proportion of a monodisperse gas in the two compartments can deviate from 1/2 and extend to a finite range.

(ii) *One-clustering state (OS)*. In this state, a stable cluster in one compartment can be observed, and over 80% of the particles staying in one compartment can be measured after the shaker is turned off.

(iii) *Granular-oscillation state (GS)*. LPs, expelled by HPs in one compartment (e.g., zone I), cluster in the other compartment (zone II) due to energy dissipation from inelastic collisions. Afterwards, without the impediment of LPs, the HPs in zone I gain sufficient energy to generate a flow of HPs to zone II, which in turn are trapped by LPs in zone II. The two stages recur, producing a granular oscillation.

(iv) *Two-clustering state (TS)*. Due to large number of particles, the balance of inflow and outflow from one specific compartment gives rise to a two-clustering state, in which particles cluster in both compartments.

(v) *Unstable-gas state (US)*. This state, situated between HS and GS (or OS) in Fig. 7, can be characterized by two scenarios: (a) that even particles do not cluster, the difference in particle numbers between two compartments is clearly visible and (b) that LPs form an unstable clustering, i.e., the clustering is apt to be broken up by incoming HPs.

Given that the number of LPs is sufficient, the possibility can be entertained that LPs can not only cluster in an empty compartment but can also trap HPs due to an increase in collisions. Figure 7, showing that GS takes place only above the clustering line, supports the need of the requirements (II) and (III) for granular oscillation. The requirement (I) has also shown its validity in Fig. 7 that granular oscillation cannot be observed for small number of HPs and larger number of LPs (dominated by OS), owing to the fact that HPs do not have sufficient energy to expel LPs.

It is found that the phase diagrams in Figs. 7(a)–7(c) share a similar topology, where the transition between TS and OS in Figs. 7(b) and 7(c) occurs at a higher N_L. For the case of small mass ratio $\bar{\mu}$ in Fig. 7(d), GS state cannot be generated even if we extend N_H to 48. In this case the BN effect is clearly observed that most LPs are covered by HPs, impeding the outflow of LPs. Furthermore, comparing Fig. 7(c) with Figs. 7(a) and 7(b) finds that the distance between the clustering line and the boundary between OS and US for higher $\bar{\mu}$ is longer than that for lower $\bar{\mu}$. This corresponds to the result obtained in Sec. IV that the change in ΔT_c depends on the mass of a larger particle added to a monodisperse gas.

VI. CONCLUSIONS

This paper has conducted a series of experiments on the phase transition of compartmentalized granular gases. By accounting for the balance of input energy and dissipation energy in granular-gas state, we obtain the information of condensation granular temperature of monodisperse gases at the gas-clustering transition from the experimentally measured relation between the critical particle number and input acceleration.

For the $M+1$ gases, an interesting result is yielded that there is an approximately linear relation (5) between the change in condensation temperature ΔT_c and the mass ratio of the intruding and background particles. The experimental data in this study identifies the proportional parameter K_c and the threshold mass ratio μ_{th}, the latter of which depends on the choice of background particles. This study manifests that the macroscopic responses of a monodisperse granular gas could be significantly different from those of the same gas with only one intruding particle added.

Moreover, the experimental phase diagrams of bidisperse granular mixtures in the space of numbers for heavier and lighter particles are constructed. These diagrams, illustrating the clustering line for LPs and the ranges of the five possible states, namely, HS, US, OS, GS, and TS, manifest the necessary requirements for generating the granular oscillation.

A final note about Fig. 7 is necessary here. If we add two or more intruding particles to a monodisperse gas, the number required for clustering will still increase but in a slow manner. The more intruding particles are involved, the more collisions are incurred, hence complicating the interactions among particles, such as the possibility of dual temperatures. Our future work aims to deal with the subject of dual temperatures, whose oscillation could be the mechanism of granular oscillation [18].

ACKNOWLEDGMENTS

This work was supported by the R.O.C. National Science Council under Grant No. NSC-97-2221-E-002-126.

[1] I. Goldhirsch and G. Zanetti, Phys. Rev. Lett. **70**, 1619 (1993).
[2] M. Oda and K. Iwashita, *Mechanics of Granular Materials* (Balkema Publishers, Netherlands, 1999).
[3] J. Duran, *Sand, Power, and Grains* (Springer, New York, 2000).
[4] M. E. Möbius, X. Cheng, G. S. Karczmar, S. R. Nagel, and H. M. Jaeger, Phys. Rev. Lett. **93**, 198001 (2004).
[5] H. Hinrichsen and D. E. Wolf, *The Physics of Granular Media* (Wiley-VCH, New York, 2004).
[6] H. M. Jaeger, S. R. Nagel, and R. P. Behringer, Rev. Mod. Phys. **68**, 1259 (1996).
[7] A. Kudrolli, M. Wolpert, and J. P. Gollub, Phys. Rev. Lett. **78**, 1383 (1997).
[8] J. Eggers, Phys. Rev. Lett. **83**, 5322 (1999).
[9] K. van der Weele, D. van der Meer, M. Versluis, and D. Lohse, Europhys. Lett. **53**, 328 (2001).
[10] D. van der Meer, K. van der Weele, and D. Lohse, Phys. Rev. E **63**, 061304 (2001).
[11] D. van der Meer, K. van der Weele, and D. Lohse, Phys. Rev. Lett. **88**, 174302 (2002).
[12] R. Mikkelsen, D. van der Meer, K. van der Weele, and D. Lohse, Phys. Rev. Lett. **89**, 214301 (2002).
[13] R. Mikkelsen, D. van der Meer, K. van der Weele, and D. Lohse, Phys. Rev. E **70**, 061307 (2004).
[14] R. Mikkelsen, K. van der Weele, D. van der Meer, M. van Hecke, and D. Lohse, Phys. Rev. E **71**, 041302 (2005).
[15] G. Costantini, D. Paolotti, C. Cattuto, and U. M. B. Marconi, Physica A **347**, 411 (2005).
[16] R. Lambiotte, J. M. Salazar, and L. Brenig, Phys. Lett. A **343**, 224 (2005).

[17] S. Viridi, M. Schmick, and M. Markus, Phys. Rev. E **74**, 041301 (2006).
[18] M. Hou, H. Tu, R. Liu, Y. Li, K. Lu, P. Y. Lai, and C. K. Chan, Phys. Rev. Lett. **100**, 068001 (2008).
[19] K. C. Chen, C. C. Li, C. H. Lin, L. M. Ju, and C. S. Yeh, J. Phys. Soc. Jpn. **77**, 084403 (2008).
[20] H. J. Schlichting and V. Nordmeier, MNU Math. Naturwiss. Unterr. **49**, 323 (1996).
[21] J. J. Brey, F. Moreno, R. García-Rojo, and M. J. Ruiz-Montero, Phys. Rev. E **65**, 011305 (2001).
[22] P. W. Atkins, *Physical Chemistry*, 6th ed. (Oxford University Press, Oxford, 1998).
[23] J. J. Brey, M. J. Ruiz-Montero, and F. Moreno, Phys. Rev. E **62**, 5339 (2000).
[24] A. Barrat and E. Trizac, Mol. Phys. **101**, 1713 (2003).
[25] A. Barrat and E. Trizac, Phys. Rev. E **66**, 051303 (2002).
[26] R. D. Wildman and D. J. Parker, Phys. Rev. Lett. **88**, 064301 (2002).
[27] J. E. Galvin, S. R. Dahl, and C. M. Hrenya, J. Fluid Mech. **528**, 207 (2005).